Voltage noise, switching rates, and multiple phase-slips in moderately damped Josephson junctions

Martin Žonda,[1] Wolfgang Belzig,[2] and Tomáš Novotný[1,*]

[1] *Department of Condensed Matter Physics, Faculty of Mathematics and Physics, Charles University in Prague, Ke Karlovu 5, 121 16 Praha 2, Czech Republic*

[2] *Fachbereich Physik, Universität Konstanz, D-78457 Konstanz, Germany*

(Dated: October 28, 2013)

We study the voltage noise properties including the switching rates and statistics of phase-slips in moderately damped Josephson junctions using a novel efficient numerical approach combining the matrix continued-fraction method with the full counting statistics. By analyzing the noise results obtained for the RCSJ model we identify different dominating components, namely the thermal noise close to equilibrium (small current-bias regime), the shot noise of (multiple) phase-slips in the intermediate range of biases and the switching noise for yet higher bias currents. We extract thus far inaccessible characteristic rates of phase-slips in the shot noise regime as well as the escape and retrapping rates in the switching regime as functions of various junction's parameters. The method can be extended and applied to other experimentally relevant Josephson junction circuits.

PACS numbers: 74.40.-n, 72.70.+m, 74.78.Na, 85.25.Cp

Introduction.— Josephson junctions (JJs) and their dynamics have been subject of intensive study ever since the discovery of the Josephson effect [1] not only because of their fascinating microscopic physical properties and high application potential but also for their ability to implement via phase dynamics elementary concepts of nonlinear dynamical systems such as chaos, multistability, and switching [2, 3]. In recent years there has been progress in fabricating unconventional meso- [4, 5] and nanoscopic [6] JJs exhibiting among other effects non-sinusoidal current-phase relations with exotic dynamics [7]. However, small junctions are more prone to the influence of environmental noise and their dynamics is inherently stochastic [8, 9]. Due to the richness of dynamical regimes even the description of conventional junctions especially in the intermediate damping regime may be challenging and one has to often resort to lengthy simulations [10].

Another side-effect of miniaturization connected to the stochastic nature of the problem is the shift of interest from just mean quantities such as the mean voltage to more elaborate statistical description including, e.g., the voltage noise in simulations [11], theory [12, 13], as well as experiment [14]. In the present paper we introduce a robust and efficient numerical method based on the matrix continued-fraction (MCF) method [3] which can be used to study the voltage noise of JJs with an arbitrary level of the phase dynamics damping. The method reveals various regimes of current-biasing the junction with the corresponding dominant voltage-noise mechanisms, including the thermal noise, multiple phase-slips (MPS), and switching processes with related escape and retrapping rates whose values are easily determined. When combined with the full counting statistics (FCS) of the phase dynamics [12] it allows us to decompose (together with a clear verification mechanism, when the decomposition is legitimate) the phase dynamics into independent elementary processes [15] constituted by MPS and find their rates.

We demonstrate the method on the paradigmatic case of the RCSJ model. However, after appropriate minor extension it is also applicable to other JJ models providing further novel results such as the voltage noise in JJs with arbitrary current-phase relations as in Ref. [5], description of the experimentally-relevant circuits with structured electromagnetic environments [13, 16], and/or frequency-dependent voltage noise for these models. Moreover, due to the phase-charge duality our results are also directly relevant for the current-noise in the nanowire quantum phase-slip circuits [17]. We defer discussion of these new results to forthcoming publications.

Model & methods.— Ideal Josephson junctions with the conventional harmonic current-phase relation $I = I_c \sin\phi$ shunted with a simple circuit environment (parallel resistance R and capacitance C; see Fig 1a) and current-biased by I_b are described by the Resistively and Capacitively Shunted Junction (RCSJ) model [18]. The Langevin equations for the phase difference $\phi(t)$ and voltage $V(t) = \frac{\hbar}{2e}\frac{d\phi(t)}{dt}$ across the junction are just the first Kirchhoff's law and the Josephson voltage-phase relation reading in the dimensionless units [2]

$$\begin{aligned} \frac{\partial v(\tau)}{\partial \tau} &= i_b - \gamma v(\tau) - \sin\phi(\tau) + \zeta(\tau), \\ v(\tau) &= \partial\phi(\tau)/\partial\tau. \end{aligned} \tag{1}$$

Dimensionless quantities are defined with help of the plasma frequency $\omega_p = \sqrt{2eI_c/\hbar C}$ and the quality factor of the circuit $Q = \omega_p RC \equiv \gamma^{-1}$ quantifying the level of damping of the phase dynamics as: junction voltage $v = \frac{QV}{I_c R}$, junction current $i = \frac{I}{I_c}$, time $\tau = \omega_p t$, tem-

perature $\Theta = \frac{2ek_BT}{\hbar I_c}$ (with the Boltzmann constant k_B), bias current $i_b = \frac{I_b}{I_c}$, and the Gaussian white noise ζ with the correlation functions $\langle\zeta(\tau)\rangle = 0$, $\langle\zeta(\tau_1)\zeta(\tau_2)\rangle = 2\gamma\Theta\delta(\tau_1 - \tau_2)$. Eqs. (1) imply the associated Fokker-Planck equation [3] for the probability distribution function $W(\phi, v, \tau)$

$$\frac{\partial}{\partial\tau}W(\phi,v;\tau) = -v\frac{\partial}{\partial\phi}W + \frac{\partial}{\partial v}\left(\gamma v + \sin\phi - i_b + \gamma\Theta\frac{\partial}{\partial v}\right)W \equiv L_{\rm FP}W(\phi,v;\tau). \tag{2}$$

We are interested in the mean voltage $\langle v\rangle = \int_0^{2\pi}\mathrm{d}\phi\int_{-\infty}^{\infty}\mathrm{d}v v W_{\rm stat}(\phi,v)$, and the (zero-frequency) voltage noise $S = \int_{-\infty}^{\infty}\mathrm{d}\tau\big(\langle v(\tau)v(0)\rangle - \langle v(\tau)\rangle\langle v(0)\rangle\big)$ in the stationary state $W_{\rm stat}(\phi,v) \equiv \lim_{\tau\to\infty}W(\phi,v;\tau)$ determined by the 2π-periodic solution (in ϕ) of the equation $L_{\rm FP}W_{\rm stat}(\phi,v) = 0$. Since the voltage autocorrelation function is expressed as [3, Sec. 7.2] $\langle v(\tau)v(0)\rangle = \int_0^{2\pi}\mathrm{d}\phi\int_{-\infty}^{\infty}\mathrm{d}v v e^{|\tau|L_{FP}}vW_{\rm stat}(\phi,v)$ the noise can be calculated by the formula $S = -2\int_0^{2\pi}\mathrm{d}\phi\int_{-\infty}^{\infty}\mathrm{d}v v R(\phi,v)$ via an auxiliary quantity $R(\phi,v)$ satisfying the equation $L_{\rm FP}R(\phi,v) = (v - \langle v\rangle)W_{\rm stat}(\phi,v)$ and conditions $R(\phi+2\pi,v) = R(\phi,v)$ and $\int_0^{2\pi}\mathrm{d}\phi\int_{-\infty}^{\infty}\mathrm{d}v R(\phi,v) = 0$ [20]. We have found both $W_{\rm stat}(\phi,v)$ and $R(\phi,v)$ numerically by the MCF method [3, Sec. 11.5] which first expresses the v-part of the equations in terms of quantum oscillator basis functions, thus obtaining a tridiagonal coupled system of ϕ-dependent differential equations (Brinkmann hierarchy). The 2π-periodic ϕ-parts are then expanded into the Fourier series and solved via the MCF as explained in the Supplemental Material [20]. The method works for an arbitrary current-phase relationship. Furthermore, using the finite-frequency generalization of the problem exactly analogous to Ref. [21], we could easily evaluate also the finite-frequency voltage noise.

An alternative method for evaluation of the zero-frequency voltage noise is to use the full counting statistics (FCS) approach pioneered in this context in Ref. [12]. The aim of that method is the calculation of the k-dependent (k is the *counting-field*) cumulant generating function (CGF) $F(k;\tau) \equiv \ln\int_{-\infty}^{\infty}\mathrm{d}\phi e^{ik\phi}\int_{-\infty}^{\infty}dvW(\phi,v;\tau)$ from a non-stationary solution $W(\phi,v;\tau)$ of Eq. (2) [3, Sec. 11.7]. For long times $\tau\to\infty$ the CGF generates *all* stationary cumulants of the voltage by derivatives with respect to k at $k = 0$ and its full k-dependence can be used for evaluation of phase-slips rates as shown below. Following the analogous derivations in Refs. [22, 23] we obtain $\lim_{\tau\to\infty}F(k;\tau)/\tau = \lambda_0(k)$, where $\lambda_0(k)$ is the

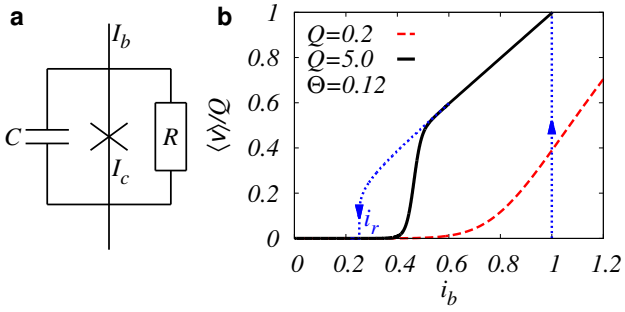

FIG. 1. (Color online) a) Circuit representation of the RCSJ model. b) $\langle v\rangle - i_b$ characteristics for a weakly-damped junction $Q = 5$ (black solid line) and a strongly-damped one $Q = 0.2$ (red dashed line). Blue dotted lines represent the hysteretic $\langle v\rangle - i_b$ characteristics for forward and backward i_b ramping of noiseless case with $Q = 5$.

counting-field-dependent eigenvalue of the full problem (2) with modified boundary condition $W_0(\phi+2\pi,v) = e^{-i2\pi k}W_0(\phi,v)$ [12] with the biggest real part (adiabatically developed with increasing k from the stationary solution $\lambda_0(k=0) = 0$). This eigenvalue can be also obtained by the MCF method as shown in the Supplemental Material [20] and yields the mean voltage $\langle v\rangle \equiv -i\lambda_0'(0)$, voltage noise $S \equiv -\lambda_0''(0)$, and similarly also the higher-order voltage cumulants. We have verified that both calculation methods give the same results for the mean voltage and noise.

$\langle v\rangle - i_b$ characteristics.— In Fig. 1b we recapitulate for completeness the known results [3] for the mean voltage by plotting $\langle v\rangle - i_b$ curves for two complementary values of the quality factor representing the strongly ($Q = 0.2$) and weakly ($Q = 5$) damped cases. While the strong damping case shows with increasing i_b a smooth crossover from the nearly zero voltage (diffusive branch [9]) to the Ohmic behavior determined by R for $i_b \gtrsim 1$, the underdamped curve exhibits a much sharper transition between the two regimes. This can be understood as the noise-induced sudden switching between two coexisting dynamical states of the underdamped junction in the noiseless (zero temperature) limit represented by the dotted blue lines in the figure revealing a strong hysteresis between the forward and backward ramping of the bias current i_b. Using the well-known mechanical analogy of the RCSJ model, which is the damped particle in the tilted washboard potential $U(\phi) = \cos\phi + i_b\phi$ (illustrated in the inset of Fig. 2a), one can easily see that the zero voltage state (locked solution) is stable up to $i_b = 1$ while a finite voltage state v_r (running solution) is stable down to the Q-dependent retrapping current $i_r(Q)$ determined by the energy balance between the energy supply by the bias current and dissipation [3]. Without noise the originally trapped "phase particle" stays locked in the potential minimum until the bias current is high

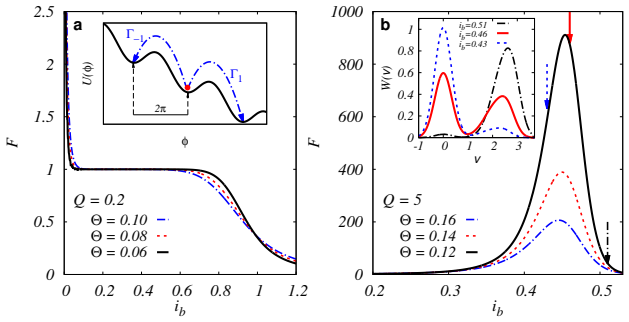

FIG. 2. (Color online) Fano factor for $Q = 0.2$ (a) and $Q = 5.0$ (b) and different temperatures Θ. Insets: mechanical analogue of Eq. (1) with $\Gamma_{1/-1}$ being the rates of the forward/backward single phase-slips (a) and bimodal stationary distribution functions plotted for bias current values marked with corresponding arrows (b).

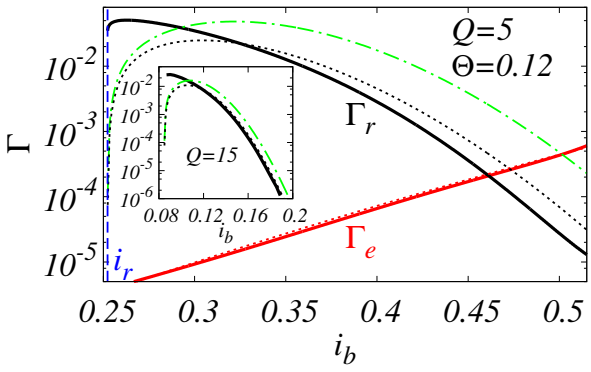

FIG. 3. (Color online) Escape rate Γ_e and retrapping rate Γ_r numerically computed from Eqs. (3) (solid lines) compared with analytical approaches (dashed lines; for details see the main text). Inset: More detailed comparison of the numerical retrapping rate (full line) with Mel'nikov's (black dashed line) and Ben-Jacob's formula (green dot-dashed line) for a junction with higher quality factor $Q = 15$.

enough to wipe off the local extremes of the potential. On the other hand, if the particle is already running, then, because of the inertia, it can still overcome the local maxima and keep running if the damping is low enough. For finite temperatures the stationary $\langle v\rangle - i_b$ characteristics in the bistability region $i_r(Q) < i_b < 1$ is the weighted average of the running and locked solutions governed by the escape and retrapping rates, which can be determined from the noise as demonstrated below.

Fano factor and switching process.— Voltage noise properties can be used to analyze the phase dynamics in far more detail. In Fig. 2 we plot the Fano factor $F \equiv S/2\pi v$ for strongly damped $Q = 0.2$ (left panel a) and weakly damped $Q = 5$ junctions (right panel b) at different temperatures. Our numerical results for the strongly damped case are very close to those for the overdamped RSJ model [12]. Because of low temperature $\Theta \ll 1$ the low-bias-current behavior for $i_b \lesssim 0.6$ can be perfectly understood by the description in terms of thermally-induced forward and backward single (i.e., by 2π) phase-slips shown in the inset of the left panel. This simple picture yields for the Fano factor in this regime $F = \coth \pi i_b/\Theta$ [12, Eq. (28)] exhibiting the characteristic divergence at $i_b = 0$ due to the finite thermal noise and the plateau at the Poissonian value of $F = 1$ for larger values of i_b. Above the critical current $i_b > 1$ the junction is in the running state and the prevailing component of the noise is the simple Johnson thermal noise of the resistor with $F = \Theta \frac{2i_b^2+1}{(i_b^2-1)^{\frac{3}{2}}}$ for $i_b \gtrsim 1 + \Theta^{2/3}$ [12, Eqs. (36),(37)].

The Fano factor vs. bias current dependence of the underdamped circuit in Fig. 2b is qualitatively different from the strongly damped case. As shown in Fig. 4a there is also the low-i_b thermal singularity in the Fano factor followed for increasing $i_b \lesssim i_r(Q)$ by a flatter part due to multiple phase-slips discussed in previous works [9, 24, 25] and studied in detail below. However, the dominant feature of the plot in Fig. 2b is the strongly temperature-dependent huge peak in the Fano factor ($F \approx 100 - 1000$) around the switching current (compare with Fig. 1b) characteristic of the dichotomous switching process. This interpretation is further supported by the inset of Fig. 2b with the voltage distribution function $W(v) \equiv \int_0^{2\pi} d\phi W_{\rm stat}(\phi, v)$ for various bias currents showing curves with well-separated double peaks corresponding to differently weighted two metastable states. The first peak centered around $v = 0$ describes the locked phase while the second one around the i_b-dependent noiseless running solution v_r reveals the running phase. Since $F \gg 1$ around the peak we can neglect noise contributions inherent to the metastable states [26] and use the average voltage $\langle v\rangle$ and Fano factor F for the evaluation of the escape rate Γ_e (from locked to running state) and retrapping rate Γ_r (from running to locked state) [23]

$$\Gamma_e = \frac{\langle v\rangle\,(v_r - \langle v\rangle)}{\pi v_r F}, \quad \Gamma_r = \frac{(v_r - \langle v\rangle)^2}{\pi v_r F}, \qquad (3)$$

which are presented in Fig. 3 as solid lines and compared with analytical predictions (dashed lines). On one hand, switching from the locked phase to the running one happens just by thermally-induced overcoming of the neighboring potential maximum and, therefore, $\Gamma_e = \frac{1}{2\pi}\left(\sqrt{\frac{\gamma^2}{4} + \sqrt{1-i_b^2}} - \frac{\gamma}{2}\right) e^{-\frac{2(i_b \arcsin i_b + \sqrt{1-i_b^2}) - \pi i_b}{\Theta}}$ is given by the Kramers escape rate from a potential well [27]. One can see that this prediction is in an excellent agreement with our numerical result. On the other hand, the retrapping problem is far more complicated

and has not been addressed in the whole parameter regime, only asymptotic solutions in various limits exist.

Two mutually inconsistent analytical approaches by Ben-Jacob et al. [28] and Mel'nikov [25, 29] were introduced for the limit of very weak damping $Q \to \infty$. In Fig. 3 we compare our results with those predictions and find a rather poor agreement with either one. With increasing Q Melnikov's approach seems to asymptotically approach our results for sufficiently large i_b as shown in the inset. Ben-Jacob's prediction on the other hand remains off which might be connected with its existing critiques [29, 30]. The origin of the obvious and persistent discrepancy between Melnikov's and our approach for i_b close to the onset of the bistability region is unclear, but we suspect it is connected with the very existence, stability, and definition of the running state for the noisy case close to the bifurcation point. In any case, the existing theories perform quite badly for the moderately damped junctions while our numerical method allows to extract the retrapping rate fast and reliably in a wide range of junction parameters, in particular for arbitrary values of the quality factor Q and bias current i_b which is the crucial ingredient for the description of switching experiments such as the recent ones in Ref. [31].

Phase-slips.— Now we turn our attention to the MPS regime of bias current smaller than the onset of the switching regime $i_b \lesssim i_r(Q)$ shown Fig. (4)a. Analogously to the overdamped case [12, 32] the solution to the Fokker-Planck equation (2) in this regime can be approximated by a weighted sum of quasi-equilibrated sharp ($\Theta \ll 1$) Gaussian distributions around the local minima $W(\phi, v; \tau) \approx \sum_m P_m(\tau) w(\phi - 2\pi m, v)$ with $w(\phi, v) = \frac{\sqrt[4]{1-i_b^2}\exp\left(-(\phi - \arcsin i_b)^2\sqrt{1-i_b^2}/2\Theta\right)\exp(-v^2/2\Theta)}{2\pi\Theta}$ [12, Eq. (22)] and time-dependent weights $P_m(\tau)$. These are *assumed* to satisfy the (Markovian) master equation

$$\begin{aligned}\frac{dP_m(\tau)}{d\tau} &= \sum_{n\neq 0}\Gamma_n P_{m-n}(\tau) - \sum_{n\neq 0}\Gamma_n P_m(\tau) \\ &\equiv \sum_n \Gamma_n P_{m-n}(\tau), \text{ with } \Gamma_0 \equiv -\sum_{n\neq 0}\Gamma_n.\end{aligned} \tag{4}$$

Here Γ_n ($n \neq 0$) are the rates of elementary MPS by $2\pi n$ (negative n correspond to backward rates against the bias).

To find the MPS rates we use the FCS methodology introduced in Ref. [12] for the RSJ model combined with the procedure of identification of elementary processes [15]. If the master equation (4) description is a good approximation of the full phase dynamics we can evaluate the CGF from it and equate that with the full CGF calculated by the MCF. We have for the approximate probability density $\exp[F(k;\tau)] \approx \sum_m P_m(\tau) e^{2\pi i k m}\tilde{w}(k) \equiv \mathcal{P}(k;\tau)\cdot\tilde{w}(k)$, with $\tilde{w}(k) = \exp\left(ik\arcsin i_b - 2\Theta k^2/\sqrt{1-i_b^2}\right)$ and $\mathcal{P}(k;\tau) \equiv \sum_m P_m(\tau) e^{2\pi i k m}$ satisfying the

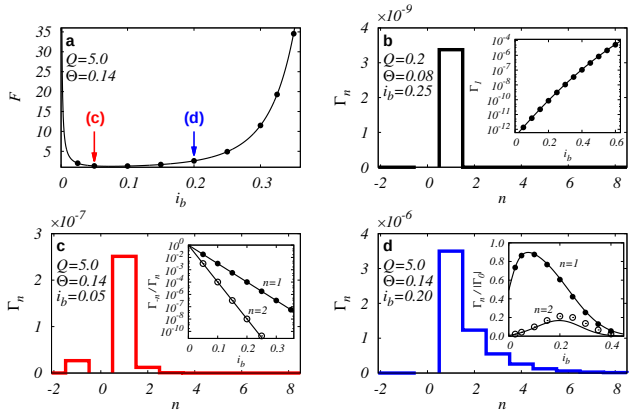

FIG. 4. (Color online) a) Detail of the $\Theta = 0.14$ Fano factor plot from Fig. 2b in the small-i_b regime where multiple phase-slips are the prevailing source of voltage noise. Full line is the Fano factor calculated from the full Fokker-Planck equation (2) while the overlapping dots are the checks evaluated via the MPS rates (see the main text). b) Single-phase-slip rate for a strongly damped junction with $Q = 0.2$. Inset: comparison of the i_b-dependence of the rate evaluated numerically (dots) and by the Kramers formula for the overdamped case (solid line). c) and d) Rates of MPS (of order n) for two values of the bias current i_b denoted in panel a) by the corresponding arrows. Insets: verification of the detailed balance condition (c) and comparison of the i_b-dependence of the first two normalized phase-slip rates (respective dots) with the Mel'nikov formula (lines) (d).

k-dependent differential equation $\frac{d\mathcal{P}(k;\tau)}{d\tau} = \left(\sum_n \Gamma_n e^{2\pi i k n} - \sum_n \Gamma_n\right)\mathcal{P}(k;\tau)$. This allows us to identify $\lambda_0(k) = \sum_n \Gamma_n (e^{2\pi i k n} - 1)$ in the MPS regime describing a mixture of independent Poissonian processes of phase-slips by $2\pi n$ whose rates can be evaluated as $\Gamma_n = \int_0^1 dk \lambda_0(k) e^{-2\pi i k n}$ for $n \neq 0$. Importantly, the method itself provides tools for checking its validity by comparing the approximate mean voltage $\langle v\rangle = 2\pi\sum_n \Gamma_n n$ and Fano factor $F = \sum_n \Gamma_n n^2 / \sum_n \Gamma_n n$ with those computed directly by the MCF method. In Fig. 4a it is explicitly shown that the two Fano-factors perfectly match up to the values of i_b where the switching process sets in (and correspondence eventually breaks down).

In Fig. 4 we plot MPS rates Γ_n for strong-damping case $Q = 0.2$ (b) and weak damping case $Q = 5$; $i_b = 0.05, 0.20$ (c, d). Only the single phase-slips are realized in the strong-damping case, which is consistent with the Fano-factor plateau at one in Fig. 2a. The dependence of Γ_1 on i_b in the regime of the plateau is plotted in the inset with dots and compared with the Kramers formula for escape across the adjacent barrier [12, 27, 33] (solid line in the inset). The behavior of the weak-damping case is much richer. The presence of multiple (double) phase-slips (alongside the single back-

ward phase-slips) is evident even for small bias currents in Fig. 4c and their importance increases with increasing bias current (Fig. 4d). The inset depicts the normalized (by $|\Gamma_0| = \sum_{n\neq 0}\Gamma_n$) rates of the single and double phase-slips as functions of i_b (dots) together with Mel'nikov's approximative asymptotic formulas valid for $Q \to \infty$ [24, 25] (solid lines in the inset). We can see reasonable agreement which analogously to Fig. 3 further improves with increasing Q. In the inset of Fig. 4c we test that the ratio $\Gamma_{-n}/\Gamma_n = \exp(-2\pi n i_b/\Theta)$ for $n = 1$, 2 satisfies the detailed balance condition with the potential drop $2\pi i_b n$ along the phase-slips of the given order n. Altogether, our method provides reliable results for the MPS rates for a wide class of junctions.

Conclusion.— To summarize, we have developed an efficient and reliable numerical scheme based on the matrix continued fraction for the analysis of phase dynamics in arbitrarily damped current-biased Josephson junctions. It allows us to study the voltage noise and, consequently, analyze in detail various transport regimes, in particular the switching regime providing us with the escape and retrapping rates and the regime of multiple phase-slips with their full characterization in terms of the corresponding rates. The method can be generalized from the RCSJ model to other experimentally relevant cases with modified circuits and/or more complicated microscopic current-phase relations as well as extended to the evaluation of the frequency-dependent voltage noise.

Acknowledgments.— We thank Pertti Hakonen, Tero Heikkilä, and Gabriel Niebler for stimulating discussions drawing our attention to this problem. We acknowledge financial support by the Czech Science Foundation via Grant No. 204/11/J042 (M.Ž. and T.N.) and by the DFG via BE 3803/5 (W.B.).

* tno@karlov.mff.cuni.cz

[1] A. Barone and G. Paternò, *Physics and Applications of the Josephson Effect* (A Willey-Interscience Publications, John Wiley & Sons, New York, Chichester, Brisbane, Toronto, Singapore, 1982); K. K. Likharev, *Dynamics of Josephson Junctions and Circuits* (Gordon and Breach, New York, 1986).
[2] R. L. Kautz, Reports on Progress in Physics **59**, 935 (1996).
[3] H. Risken, *The Fokker-Planck Equation, 2nd ed.* (Springer-Verlag, Berlin, Heidelberg, 1989).
[4] A. I. Buzdin, Rev. Mod. Phys. **77**, 935 (2005).
[5] H. Sickinger, A. Lipman, M. Weides, R. G. Mints, H. Kohlstedt, D. Koelle, R. Kleiner, and E. Goldobin, Phys. Rev. Lett. **109**, 107002 (2012).
[6] S. De Franceschi, L. Kouwenhoven, C. Schönenberger, and W. Wernsdorfer, Nat Nano **5**, 703 (2010).
[7] E. Goldobin, R. Kleiner, D. Koelle, and R. G. Mints, Physical Review Letters **111**, 057004 (2013).
[8] J. M. Martinis and R. L. Kautz, Phys. Rev. Lett. **63**, 1507 (1989).
[9] R. L. Kautz and J. M. Martinis, Phys. Rev. B **42**, 9903 (1990).
[10] J. C. Fenton and P. A. Warburton, Phys. Rev. B **78**, 054526 (2008).
[11] R. F. Voss, Journal of Low Temperature Physics **42**, 151 (1981).
[12] D. S. Golubev, M. Marthaler, Y. Utsumi, and G. Schön, Phys. Rev. B **81**, 184516 (2010).
[13] M. Žonda and T. Novotný, Physica Scripta **2012**, 014023 (2012).
[14] P. Hakonen, private communication.
[15] M. Vanević, Y. V. Nazarov, and W. Belzig, Physical Review Letters **99**, 076601 (2007); Physical Review B **78**, 245308 (2008); C. Padurariu, F. Hassler, and Y. V. Nazarov, Physical Review B **86**, 054514 (2012).
[16] P. Joyez, D. Vion, M. Götz, M. Devoret, and D. Esteve, Journal of Superconductivity **12**, 757 (1999).
[17] C. H. Webster, J. C. Fenton, T. T. Hongisto, S. P. Giblin, A. B. Zorin, and P. A. Warburton, Phys. Rev. B **87**, 144510 (2013).
[18] D. E. McCumber, Journal of Applied Physics **39**, 3113 (1968); W. C. Stewart, Applied Physics Letters **12**, 277 (1968).
[19] C. Flindt, T. Novotný, and A.-P. Jauho, Phys. Rev. B **70**, 205334 (2004).
[20] M. Žonda, W. Belzig, and T. Novotný, "Supplemental material".
[21] C. Flindt, T. Novotný, and A.-P. Jauho, Physica E **29**, 411 (2005).
[22] D. A. Bagrets and Y. V. Nazarov, Phys. Rev. B **67**, 085316 (2003).
[23] C. Flindt, T. Novotný, and A.-P. Jauho, Europhys. Lett. **69**, 475 (2005).
[24] V. I. Mel'nikov, Zh. Eksp. Teor. Fiz. **18**, 1429 (1985).
[25] V. I. Mel'nikov, Physics Reports **209**, 1 (1991).
[26] A. N. Jordan and E. V. Sukhorukov, Phys. Rev. Lett. **93**, 260604 (2004).
[27] P. Hänggi, P. Talkner, and M. Borkovec, Rev. Mod. Phys. **62**, 251 (1990).
[28] E. Ben-Jacob, D. J. Bergman, B. J. Matkowsky, and Z. Schuss, Phys. Rev. A **26**, 2805 (1982).
[29] V. I. Mel'nikov, Zh. Eksp. Teor. Fiz. **93**, 2037 (1987).
[30] P. Jung and H. Risken, Zeitschrift fur Physik B Condensed Matter **54**, 357 (1984).
[31] J. Männik, S. Li, W. Qiu, W. Chen, V. Patel, S. Han, and J. E. Lukens, Physical Review B **71**, 220509 (2005); V. M. Krasnov, T. Bauch, S. Intiso, E. Hürfeld, T. Akazaki, H. Takayanagi, and P. Delsing, Physical Review Letters **95**, 157002 (2005); J. M. Kivioja, T. E. Nieminen, J. Claudon, O. Buisson, F. W. J. Hekking, and J. P. Pekola, Physical Review Letters **94**, 247002 (2005); V. M. Krasnov, T. Golod, T. Bauch, and P. Delsing, Physical Review B **76**, 224517 (2007); A. Murphy, P. Weinberg, T. Aref, U. C. Coskun, V. Vakaryuk, A. Levchenko, and A. Bezryadin, Physical Review Letters **110**, 247001 (2013).
[32] K. J. Challis and M. W. Jack, Physical Review E **87**, 052102 (2013).
[33] H. A. Kramers, Physica **7**, 284 (1940).

Supplemental Material for "Voltage noise, switching rates, and multiple phase-slips in moderately damped Josephson junctions"

Martin Žonda, Wolfgang Belzig, and Tomáš Novotný

Aim of this supplemental material is to provide an introduction to a reader not familiar with the methods used in our paper, namely the Matrix Continued-Fraction (MCF) method and the full counting statistics (FCS).

Matrix Continued-Fraction Method

In the paper we discussed a numerical solution of the dimensionless Langevin equations

$$\begin{aligned} \frac{\partial v(\tau)}{\partial \tau} &= i_b - \gamma v(\tau) - \sin\phi(\tau) + \zeta(\tau), \\ v(t) &= \partial\phi/\partial\tau, \end{aligned} \tag{1}$$

with the associated Fokker-Planck equation for the probability distribution function $W(\phi, v, \tau)$

$$\begin{aligned} \frac{\partial}{\partial\tau}W(\phi, v; \tau) &= -v\frac{\partial}{\partial\phi}W + \frac{\partial}{\partial v}\left(\gamma v + \sin\phi - i_b + \gamma\Theta\frac{\partial}{\partial v}\right)W \\ &\equiv L_{\mathrm{FP}}W(\phi, v; \tau). \end{aligned} \tag{2}$$

Our first goal was to calculate the mean voltage

$$\langle v\rangle = \int_0^{2\pi} \mathrm{d}\phi \int_{-\infty}^{\infty} \mathrm{d}v v W_{\mathrm{stat}}(\phi, v), \tag{3}$$

and the (zero-frequency) voltage noise

$$S = \int_{-\infty}^{\infty} \mathrm{d}\tau \big(\langle v(\tau)v(0)\rangle - \langle v(\tau)\rangle\langle v(0)\rangle\big) \tag{4}$$

in the stationary state $W_{\mathrm{stat}}(\phi, v) \equiv \lim_{\tau\to\infty} W(\phi, v; \tau)$ determined by the 2π-periodic solution (in ϕ) of the equation

$$L_{\mathrm{FP}}W_{\mathrm{stat}}(\phi, v) = 0. \tag{5}$$

We have used the MCF method [1] to obtain the numerical solution for the stationary distribution function and our explanation closely follows that work. The operator L_{FP} can be partitioned into irreversible L_i and reversible L_r operators

$$L_i = \gamma\frac{\partial}{\partial v}\left(v + \Theta\frac{\partial}{\partial v}\right), \tag{6}$$

$$L_r = -v\frac{\partial}{\partial\phi}W - U'(\phi)\frac{\partial}{\partial v}, \tag{7}$$

with

$$U(\phi) = i_b\phi + \cos\phi. \tag{8}$$

The irreversible operator L_i can be mapped onto the Hamilton operator of the linear harmonic oscillator via a suitable similarity transformation

$$\widetilde{L_i} = \exp\left[\frac{v^2}{4\Theta}\right] L_i \exp\left[-\frac{v^2}{4\Theta}\right] = -\gamma b^\dagger b, \tag{9}$$

where the creation $b^\dagger$ and annihilation b operators were introduced

$$b^\dagger = -\sqrt{\Theta}\frac{\partial}{\partial v} + \frac{v}{2\sqrt{\Theta}}, \tag{10}$$

$$b = \sqrt{\Theta}\frac{\partial}{\partial v} + \frac{v}{2\sqrt{\Theta}}. \tag{11}$$

For the reversible operator we consequently get

$$\widetilde{L_r} = \exp\left[\frac{v^2}{4\Theta}\right] L_r \exp\left[-\frac{v^2}{4\Theta}\right] = -b^\dagger D_2 - bD_1, \tag{12}$$

with ϕ- dependent operators

$$D_1 = \sqrt{\Theta}\frac{\partial}{\partial \phi}, \tag{13}$$

$$D_2 = \sqrt{\Theta}\frac{\partial}{\partial \phi} - \frac{U'(\phi)}{\sqrt{\Theta}}. \tag{14}$$

Altogether we have

$$L_{\rm FP} = \exp\left[-\frac{v^2}{4\Theta}\right]\left(-\gamma b^\dagger b - b^\dagger D_2 - bD_1\right)\exp\left[\frac{v^2}{4\Theta}\right]. \tag{15}$$

After these manipulations it is convenient to expand the v part of distribution function $W(\phi, v; \tau)$ into the Hermite oscillator functions $\psi_n(v)$

$$W(\phi, v; \tau) = \psi_0(v)\sum_n c_n(\phi; \tau)\psi_n(v), \tag{16}$$

which are given by

$$\psi_0(v) = e^{-\frac{1}{2}(\kappa v)^2}/\sqrt{\kappa\sqrt{\pi}},$$
$$\psi_n(v) = \left(b^\dagger\right)^n \psi_0(v)/\sqrt{n!},$$

with $\kappa = 1/\sqrt{2\Theta}$ or in terms of Hermite polynomials $H_n(\kappa v)$ used in quantum mechanics

$$\psi_n(v) = H_n(\kappa v)\, e^{-\frac{1}{2}(\kappa v)^2}/\sqrt{n! 2^n \kappa\sqrt{\pi}}. \tag{17}$$

The oscillator functions are the eigenfunctions of the irreversible part of the $L_{\rm FP}$ operator and have the correct boundary conditions ($\lim_{v\to\pm\infty} W(\phi, v; \tau) = 0$). Consequently,

$$\int_{-\infty}^{\infty} dv\, W(\phi, v; \tau) = c_0(\phi; \tau), \tag{18}$$

$$\int_{-\infty}^{\infty} dv\, vW(\phi, v; \tau) = \sqrt{\Theta}c_1(\phi; \tau), \tag{19}$$

and the initial values of the ϕ-part coefficients read

$$c_n(\phi; 0) = \int_{-\infty}^{\infty} dv\, \psi_n\psi_0^{-1}W(\phi, v; 0). \tag{20}$$

Using Eq. (9)-(16) the Brinkman hierarchy, equivalent to the Fokker-Planck equation (2), can be constructed

$$-\sqrt{m}D_2 c_{m-1}(\phi; \tau) - \gamma m c_m(\phi; \tau) - \sqrt{m+1}D_1 c_{m+1}(\phi, ; \tau) = \frac{\partial}{\partial \tau}c_m(\phi; \tau). \tag{21}$$

Stationary Distribution Function and Average Voltage

Because of the chosen potential Eq. (8) the Fokker-Planck operator Eq. (15) commutes with the translation operator T defined by

$$T\,W(\phi,v;\tau)=W(\phi+2\pi,v;\tau), \tag{22}$$

therefore the eigenfunctions $\varphi_n(k,\phi,v)$ of operator $L_{\rm FP}$ and its adjoint operator $L^+_{\rm FP}$

$$\begin{aligned}L_{\rm FP}\varphi_n(k,\phi,v)&=\lambda_n(k)\varphi_n(k,\phi,v),\\ L^+_{\rm FP}\varphi^+_n(k,\phi,v)&=\lambda_n(k)\varphi^+_n(k,\phi,v),\end{aligned}$$

with $k\in(-1/2,1/2]$ restricted to the first Brillouin zone can be written in the form of the Bloch waves

$$\begin{aligned}\varphi_n(k,\phi,v)&=e^{-ik\phi}u_n\left(k,\phi,v\right),\ u_n(k,\phi,v)=u_n(k,\phi+2\pi,v),\\ \varphi^+_n(k,\phi,v)&=e^{ik\phi}u^+_n\left(k,\phi,v\right),\ u^+_n(k,\phi,v)=u^+_n(k,\phi+2\pi,v).\end{aligned} \tag{23}$$

Consequently, the solutions of the Eq. (5) can be chosen to be

$$W_{\rm stat}(\phi,v)=e^{-ik\phi}u\left(k,\phi,v\right), \tag{24}$$

with $e^{-i2\pi k}$, $-1/2<k\le 1/2$, being the eigenvalues of the translation operator T. The stationary expansion coefficients $c_n(\phi)\equiv\lim_{\tau\to\infty}c_n(\phi;\tau)$ must therefore have the form

$$c_n(\phi)=e^{-ik\phi}u_n(k,\phi),\quad u_n(k,\phi)=u_n(k,\phi+2\pi). \tag{25}$$

Note that the stationary form of the Brinkman hierarchy Eq. (21) reads

$$\begin{aligned}\sqrt{1}D_1c_1(\phi)&=0\\ \sqrt{1}D_2c_0(\phi)+1\gamma c_1(\phi)+\sqrt{2}D_1c_2(\phi)&=0\\ \sqrt{2}D_2c_1(\phi)+2\gamma c_2(\phi)+\sqrt{3}D_1c_3(\phi)&=0\\ &\vdots\end{aligned} \tag{26}$$

from which it is obvious that $c_1(\phi)=c_1=\text{const}$. Since c_1 is related by Eq. (19) to the mean voltage being generically non-zero, the constancy of c_1 implies $k=0$ for the stationary solution. Thus, the stationary distribution function is periodic

$$W_{\rm stat}(\phi,v)=W_{\rm stat}(\phi+2\phi,v),\quad c_n(\phi)=c_n(\phi+2\pi) \tag{27}$$

and can be normalized in one period

$$\int\limits_{-\infty}^{\infty}dv\int\limits_0^{2\pi}d\phi\,W_{\rm stat}(\phi,v)=\int\limits_0^{2\pi}d\phi c_0(\phi)=1, \tag{28}$$

$$\langle v\rangle=\int\limits_{-\infty}^{\infty}dv\int\limits_0^{2\pi}d\phi\,vW_{\rm stat}(\phi,v)=\sqrt{\Theta}\int\limits_0^{2\pi}d\phi c_1(\phi)=\sqrt{\Theta}2\pi c_1. \tag{29}$$

To solve Eq. (5) for the periodic coefficients $c_m(\phi)$ we have used the Fourier expansion

$$c_m(\phi)=\frac{1}{\sqrt{2\pi}}\sum_p c_m^p\,e^{ip\phi}, \tag{30}$$

allowing us to define the matrix elements of operators $\mathcal{D}^+_m,\mathcal{D}_m,\mathcal{D}^-_m$

$$\begin{aligned}\left(\mathcal{D}^+_m\right)^{pq}&\equiv-\frac{\sqrt{m+1}}{2\pi}\int\limits_0^{2\pi}d\phi\,e^{-ip\phi}D_1e^{iq\phi}=-i\sqrt{m+1}\sqrt{\Theta}p\,\delta_{p,q},\\ \left(\mathcal{D}_m\right)^{pq}&\equiv-\gamma m\,\delta_{p,q},\\ \left(\mathcal{D}^-_m\right)^{pq}&\equiv-\frac{\sqrt{m}}{2\pi}\int\limits_0^{2\pi}d\phi\,e^{-ip\phi}D_2e^{iq\phi}=-i\sqrt{m}\sqrt{\Theta}\left[\left(p+i\frac{i_b}{\Theta}\right)\,\delta_{p,q}+\frac{\delta_{p,q-1}-\delta_{p,q+1}}{2\Theta}\right],\end{aligned} \tag{31}$$

which can be used to recast the Eq. (26) into the form of a vector tridiagonal recurrence relation

$$\mathcal{D}_m^- \mathbf{c}_{m-1} + \mathcal{D}_m \mathbf{c}_m + \mathcal{D}_m^+ \mathbf{c}_{m+1} = 0, \tag{32}$$

where $\mathbf{c}_m$ is a time-independent vector of expansion coefficients c_m^p from Eq. (30)

$$\mathbf{c}_m = \begin{pmatrix} \vdots \\ c_m^{-1} \\ c_m^0 \\ c_m^1 \\ \vdots \end{pmatrix}. \tag{33}$$

To solve the relation (32) we defined matrices $\mathcal{S}_m$ obeying

$$\mathbf{c}_{m+1} = \mathcal{S}_m \mathbf{c}_m, \quad \mathbf{c}_m = \mathcal{S}_m^{-1} \mathbf{c}_{m+1}, \tag{34}$$

which transforms the Eq. (32) into

$$\mathcal{D}_m^- \mathcal{S}_{m-1}^{-1} \mathbf{c}_m + \mathcal{D}_m \mathbf{c}_m + \mathcal{D}_m^+ \mathcal{S}_m \mathbf{c}_m = 0, \tag{35}$$

and consequently a matrix continued-fraction structure can be constructed

$$\mathcal{S}_{m-1} = -\left(\mathcal{D}_m + \mathcal{D}_m^+ \mathcal{S}_m\right)^{-1} \mathcal{D}_m^-. \tag{36}$$

By truncating the recurrence at $m = M$, i.e., setting $\mathbf{c}_{m>M} = 0$ in Eq. (32) and using the normalization condition (28) together with the fact that the coefficient c_1 is constant we obtain for the vector $\mathbf{c}_0$

$$c_0^p = \frac{1}{\sqrt{2\pi}} \frac{\left(\mathcal{S}_0^{-1}\right)^{p0}}{\left(\mathcal{S}_0^{-1}\right)^{00}}. \tag{37}$$

All other vectors $\mathbf{c}_m$ follow from Eq. (34). In particular, the average voltage reads

$$\langle v \rangle = \sqrt{\Theta} 2\pi c_1 \equiv \sqrt{2\pi\Theta} c_1^0 = \frac{\sqrt{\Theta}}{\left(\mathcal{S}_0^{-1}\right)^{00}}. \tag{38}$$

Voltage noise

Computation of the voltage noise is more complicated. The general formula for the frequency dependent voltage noise reads

$$S(\omega) = \int_{-\infty}^{\infty} \mathrm{d}\tau e^{i\omega\tau} \left(\langle v(\tau) v(0) \rangle - \langle v(\tau) \rangle \langle v(0) \rangle \right) \tag{39}$$

and the voltage autocorrelation function can be expressed as [1, Sec. 7.2]

$$\langle v(\tau) v(0) \rangle = \int_0^{2\pi} \mathrm{d}\phi \int_{-\infty}^{\infty} \mathrm{d}v \, v e^{|\tau| L_{FP}} v W_{\mathrm{stat}}(\phi, v). \tag{40}$$

After introducing the convergence factors $\omega \to \omega + i0$ for $\tau > 0$ and $\omega \to \omega - i0$ for $\tau < 0$ we get

$$S(\omega) = \int_0^{2\pi} \mathrm{d}\phi \int_{-\infty}^{\infty} \mathrm{d}v \, v \left(\frac{1}{i\omega - L_{\mathrm{FP}}} - \frac{1}{i\omega + L_{\mathrm{FP}}} \right) v W_{\mathrm{stat}}(\phi, v). \tag{41}$$

Since we are interested in the limit $\omega \to 0$ and L_{FP} is singular (due to the existence of the stationary state), performing the limit is somewhat tricky. It can be done, however, as explained in detail in Ref. [2, Sec. IIIB] and the the voltage noise can be evaluated as

$$S = -2\int_0^{2\pi} \mathrm{d}\phi \int_{-\infty}^{\infty} \mathrm{d}v v R(\phi, v) \tag{42}$$

with the help of an auxiliary quantity $R(\phi, v)$ (pseudoinverse of the Fokker-Planck operator) satisfying the equation

$$L_{\mathrm{FP}} R(\phi, v) = (v - \langle v \rangle) W_{\mathrm{stat}}(\phi, v), \tag{43}$$

and conditions $R(\phi + 2\pi, v) = R(\phi, v)$ (periodicity) and $\int_0^{2\pi} \mathrm{d}\phi \int_{-\infty}^{\infty} \mathrm{d}v R(\phi, v) = 0$ (fixing one out of infinitely many solutions of Eq. (43), see [2, Sec. IIIE]). We have obtained the numerical solution of Eq. (43) analogously to the solution of Eq. (5) — the main difference is that for Eq. (43) the vector tridiagonal recurrence relation has a right-hand side

$$\mathcal{D}_m^- \mathbf{a}_{m-1} + \mathcal{D}_m \mathbf{a}_m + \mathcal{D}_m^+ \mathbf{a}_{m+1} = \alpha_m, \tag{44}$$

with $\mathbf{a}_m$ being a time-independent vector of expansion coefficients a_m^p of $R(\phi, v)$ obtained in the same procedure as coefficients c_m^p in Eq. (30) for $W_{\mathrm{stat}}(\phi, v)$ and

$$\alpha_m = \sqrt{\Theta m}\mathbf{c}_{m-1} - \langle v \rangle \mathbf{c}_m + \sqrt{\Theta(m+1)}\mathbf{c}_{m+1}. \tag{45}$$

Introducing the correction vectors g_m satisfying

$$\mathbf{a}_{m+1} = \mathcal{S}_m \mathbf{a}_m + g_m, \tag{46}$$

the Eq. (44) gives a recurrent prescription for their evaluation

$$g_{m-1} = -\left(\mathcal{D}_m + \mathcal{D}_m^+ \mathcal{S}_m\right)^{-1} \left(\mathcal{D}_m^+ g_m - \alpha_m\right). \tag{47}$$

After truncation of Eq. (44) at $m = M$ and using the proper normalization conditions together with Eq. (46) this recurrent relation is used to obtain the auxiliary quantity $R(\phi, v)$ and, consequently, the voltage noise.

Non-stationary solution

As we are interested in the statistics of $2\pi n$ phase-slips we have to consider also the non-periodic solutions of the Fokker-Planck equation in the non-stationary case. Recalling the expansion Eq. (16) and the Brinkman hierarchy Eq. (21) it is clear that to make use of the MCF method we need a complete set of functions $\varphi^p(\phi)$ in which the coefficients $c_m(\phi; \tau)$ can be expanded. One of the possibilities is to use the eigenfunctions Eq. (23) or equivalently make use of the Floquet theorem as an ansatz for the non-periodic solution

$$W(\phi, v; \tau) = \int_{-\frac{1}{2}}^{\frac{1}{2}} dk\, \mathcal{W}(k, \phi, v; \tau) e^{-ik\phi}, \tag{48}$$

where $\mathcal{W}(k, \phi, v; \tau)$ is periodic in ϕ with period 2π and k is restricted to the first Brillouin zone. Similarly as was done before for the distribution function the function $\mathcal{W}(k, \phi, v; \tau)$ can be expanded in

$$\mathcal{W}(k, \phi, v; \tau) = \psi_0(v) \sum_n \sum_p c_n^p(k; \tau) e^{ip\phi} \psi_n(v), \tag{49}$$

yielding the complete set of functions in which the coefficients are expanded

$$\varphi^p(k, \phi) = \frac{1}{\sqrt{2\pi}} e^{i(p-k)\phi}. \tag{50}$$

Using time-dependent vectors $\mathbf{c}_m(k; \tau)$ of expansion coefficients $c_m^p(k, \tau)$, Eq. (21) changes to

$$\mathcal{D}_m^- \mathbf{c}_{m-1}(k; \tau) + \mathcal{D}_m \mathbf{c}_m(k; \tau) + \mathcal{D}_m^+ \mathbf{c}_{m+1}(k; \tau) = \dot{\mathbf{c}}_m(k; \tau), \tag{51}$$

with

$$\left(\mathcal{D}_m^+\right)^{pq} = -\frac{\sqrt{m+1}}{2\pi}\int_0^{2\pi} d\phi\, e^{-i(p-k)\phi} D_1 e^{i(p-k)\phi} = -i\sqrt{m+1}\sqrt{\Theta}(p-k)\,\delta_{p,q}, \tag{52}$$

$$\left(\mathcal{D}_m\right)^{pq} = -\gamma m\,\delta_{p,q}, \tag{53}$$

$$\left(\mathcal{D}_m^-\right)^{pq} = -\frac{\sqrt{m}}{2\pi}\int_0^{2\pi} d\phi\, e^{-i(p-k)\phi} D_2 e^{i(p-k)\phi} = -i\sqrt{m}\sqrt{\Theta}\left[\left(p-k+i\frac{i_b}{\Theta}\right)\,\delta_{p,q} + \frac{\delta_{p,q-1}-\delta_{p,q+1}}{2\Theta}\right]. \tag{54}$$

One way to solve this initial value problem is to use the Laplace transform

$$\tilde{\mathbf{c}}_m(k;s) = \int_0^\infty d\tau\, \mathbf{c}_m(k;\tau)\, e^{-s\tau}, \tag{55}$$

which turns Eq. (21) into

$$\mathcal{D}_m^-\tilde{\mathbf{c}}_{m-1}(k;s) + \tilde{\mathcal{D}}_m\tilde{\mathbf{c}}_m(k;s) + \mathcal{D}_m^+\tilde{\mathbf{c}}_{m+1}(k;s) = -\mathbf{c}_m(k;0), \tag{56}$$

with

$$\tilde{\mathcal{D}}_m = \mathcal{D}_m - sI. \tag{57}$$

This equation can be solved analogously to the solution of Eq. (44) and the resulting s-dependent quantities can be inverse Laplace transformed to the time domain. Alternatively, one can use the homogeneous version of Eq. (56) for determining the eigenvalues of the Fokker-Planck operator from the condition

$$\mathrm{Det}\left[\mathcal{D}_m - \lambda I + \mathcal{D}_m^-\mathcal{S}_{m-1}^{-1}(\lambda) + \mathcal{D}_m^+\mathcal{S}_m(\lambda)\right] = 0 \tag{58}$$

and, consequently, for finding the nonstationary solution by the spectral decomposition

$$W(\phi,v;\tau) = \int_{-1/2}^{1/2} dk \sum_n e^{-ik\phi} u_n\left(k,\phi,v\right) e^{\lambda_n(k)\tau}. \tag{59}$$

The advantage of the eigenfunction expansion is that the transition probability from state ϕ', v' to ϕ, v has a simple form [1, Sec. 11.7]

$$P(\phi,v;\tau|\phi',v',0) = \int_{-1/2}^{1/2} dk \sum_n u_n^+(k,\phi',v')u_n(k,\phi,v)e^{-ik(\phi-\phi')}e^{\lambda_n(k)\tau}, \tag{60}$$

whose long time $\tau\to\infty$ asymptotics is easily determined as (we assume that the eigenvalue $\lambda_0(k)$ with the highest real part corresponding to the stationary solution with $\lambda_0(0)=0$ is separated by a finite gap from other eigenvalues $\Re[\lambda_n(k)-\lambda_0(k)]<0$ for $n\geq 1$)

$$P(\phi,v;\tau\to\infty|\phi',v',0) \approx \int_{-1/2}^{1/2} dk\, u_0^+(k,\phi',v')u_0(k,\phi,v)e^{-ik(\phi-\phi')}e^{\lambda_0(k)\tau}, \tag{61}$$

or

$$W(\phi,v;\tau\to\infty) = \int_{-1/2}^{1/2} dk\, I_0(k)u_0(k,\phi,v)e^{-ik\phi}e^{\lambda_0(k)\tau}, \tag{62}$$

with $I_0(k)$ being determined solely by the initial condition.

Full Counting Statistics

As pointed out in the paper an alternative method for the evaluation of the voltage cumulants is to use the full counting statistics (FCS) approach pioneered in this context in Ref. [3]. The aim of that method is the calculation of the k-dependent (k is the *counting-field*) cumulant generating function (CGF) $F(k;\tau) \equiv \ln \int_{-\infty}^{\infty} \mathrm{d}\phi e^{ik\phi} \int_{-\infty}^{\infty} dv W(\phi, v; \tau)$ from a non-stationary solution $W(\phi, v; \tau)$ of Eq. (2) [1, Sec. 11.7]. Using the Floquet theorem and Eq. (62) once again the CGF can be written as

$$\begin{aligned}
\exp[F(k;\tau\to\infty)] &= \int_{-\infty}^{\infty} d\phi \int_{-\infty}^{\infty} dv W(\phi, v; \tau\to\infty) e^{ik\phi} \\
&\approx \int_{-\infty}^{\infty} d\phi \int_{-\infty}^{\infty} dv \int_{-\frac{1}{2}}^{\frac{1}{2}} dl\, I_0(l) u_0(l,\phi,v) e^{\lambda_0(l)\tau} e^{i(k-l)\phi} \\
&= \frac{1}{\sqrt{2\pi}} \int_{-\infty}^{\infty} d\phi \int_{-\frac{1}{2}}^{\frac{1}{2}} dl\, I_0(l) \sum_p c_0^p(l) e^{i(p-l+k)\phi} e^{\lambda_0(l)\tau} \\
&= \frac{1}{\sqrt{2\pi}} \int_{-\frac{1}{2}}^{\frac{1}{2}} dl\, I_0(l) e^{\lambda_0(l)\tau} \sum_p c_0^p(l) \lim_{N\to\infty} \sum_{n=-N}^{N} \left\{ \int_{2\pi n}^{2\pi(n+1)} d\phi\, e^{i(p-l+k)\phi} \right\} \\
&= \frac{1}{\sqrt{2\pi}} \int_{-\frac{1}{2}}^{\frac{1}{2}} dl\, I_0(l) e^{\lambda_0(l)\tau} \sum_p c_0^p(l) \int_0^{2\pi} d\phi\, e^{i(p-l+k)\phi} \lim_{N\to\infty} \sum_{n=-N}^{N} e^{2\pi i(p-l+k)n} \\
&= \frac{1}{\sqrt{2\pi}} \int_{-\frac{1}{2}}^{\frac{1}{2}} dl\, I_0(l) e^{\lambda_0(l)\tau} \sum_p c_0^p(l) \Xi(p-l+k) \int_0^{2\pi} d\phi\, e^{i(p-l+k)\phi}.
\end{aligned} \tag{63}$$

As both l and k are from the first Brillouin zone and p is an integer the use of the Dirac comb function $\Xi(x) = \sum_{n\in Z} \delta(x-n)$ implies $p=0$ and $k=l$ which leads to

$$F(k;\tau\to\infty) = \lambda_0(k)\tau + \ln\sqrt{2\pi} I_0(k) c_0^0(k). \tag{64}$$

The second term depends on the initial state of the system and is irrelevant in the long time limit. Zero-frequency n-th cumulant of v follows from [3]

$$C_n = \lim_{\tau\to\infty} \frac{(-i)^n}{\tau} \left.\frac{\partial^n F(k,\tau)}{\partial k^n}\right|_{k=0} = (-i)^n \left.\frac{\partial^n \lambda_0(k)}{\partial k^n}\right|_{k=0}. \tag{65}$$

* tno@karlov.mff.cuni.cz

[1] H. Risken, *The Fokker-Planck Equation, 2nd ed.* (Springer-Verlag, Berlin, Heidelberg, 1989).
[2] C. Flindt, T. Novotný, and A.-P. Jauho, Phys. Rev. B **70**, 205334 (2004).
[3] D. S. Golubev, M. Marthaler, Y. Utsumi, and G. Schön, Phys. Rev. B **81**, 184516 (2010).